Environmental Science & Technology

pubs.acs.org/est

Article

Methane Emissions from Superemitting Coal Mines in Australia Quantified Using TROPOMI Satellite Observations

Pankaj Sadavarte,* Sudhanshu Pandey, Joannes D. Maasakkers, Alba Lorente, Tobias Borsdorff, Hugo Denier van der Gon, Sander Houweling, and Ilse Aben

Cite This: *Environ. Sci. Technol.* 2021, 55, 16573−16580

Read Online

ACCESS | Metrics & More | Article Recommendations | Supporting Information

ABSTRACT: Two years of satellite observations were used to quantify methane emissions from coal mines in Queensland, the largest coal-producing state in Australia. The six analyzed surface and underground coal mines are estimated to emit 570 ± 98 Gg a^{-1} in 2018−2019. Together, they account for 7% of the national coal production while emitting 55 ± 10% of the reported methane emission from coal mining in Australia. Our results indicate that for two of the three locations, our satellite-based estimates are significantly higher than reported to the Australian government. Most remarkably, 40% of the quantified emission came from a single surface mine (Hail Creek) located in a methane-rich coal basin. Our findings call for increased monitoring and investment in methane recovery technologies for both surface and underground mines.

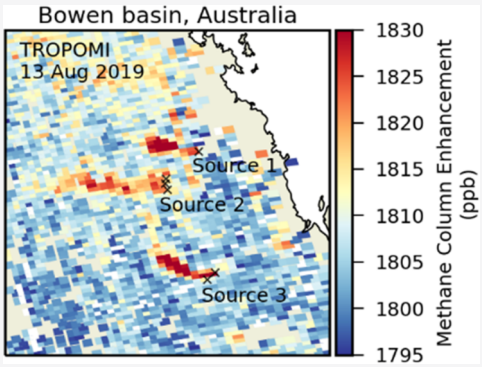

KEYWORDS: *underground mines, surface mines, source rate, emission inventory, superemitters*

INTRODUCTION

Methane (CH_4) is the second most important greenhouse gas and is responsible for 25% of the anthropogenic radiative forcing in the atmosphere.[1] Due to its shorter atmospheric lifetime (~12 years) compared to CO_2 and higher greenhouse warming potential, the mitigation of methane emissions is an efficient method to tackle near-term climate warming.[2] The current methane growth rate, however, challenges existing climate policies, including the Paris Agreement (PA), and will ask for additional reductions on top of what is already foreseen to attain the PA goals.[3] To do this in an efficient manner, an improved understanding and quantification of anthropogenic methane emissions are of vital importance.

The fossil fuel industry, including oil/gas (O/G) production and coal mining, accounts for one-third of the total anthropogenic methane emission.[4,5] Coal mining is responsible for about 12% of total anthropogenic methane emissions,[4,5] with 90% coming from underground mines.[6] The recent global methane budget suggests an increase of 38% (12 Tg) in emissions from coal mines between 2000−2009 and 2017,[4,7] most likely due to the increase in global coal production. Methane emissions from coal mines have been quantified using atmospheric measurements from ground-based and aircraft campaigns.[8,9] Space-borne remote-sensing instruments have been used to detect and quantify methane emissions on a regional scale and can provide a measurement-based integral quantification of large point sources.[10−13] Recent developments in space-borne instruments with subkilometer pixel resolution have made identification and quantification of emissions from individual oil and gas facilities and coal mine shafts possible.[14,15] However, these high-resolution satellites have limited spatial coverage as they tend to only observe targeted areas.[15]

Here, we use satellite observations of the TROPOspheric Monitoring Instrument (TROPOMI) onboard the Copernicus Sentinel-5 Precursor (S-5P) satellite, launched on 13 October 2017. It is a push broom imaging spectrometer in a sun-synchronous orbit providing daily global methane columns (XCH_4) with a local overpass time at 13:30.[16] The daily global coverage combined with a fine spatial resolution of 7 × 7 km^2 (7 × 5.5 km^2 since August 2019) of TROPOMI enables the detection of superemitters of methane in a single overpass.[12,14,17]

In this study, we quantify fugitive methane plumes from coal mines observed with TROPOMI over Queensland state in Australia (Figure 1). We use two years (2018−2019) of clear-sky column-averaged methane (XCH_4) observations with the data-driven cross-sectional flux method (CSF) to estimate emissions. This method has been used in previous studies to quantify emissions from point sources using satellite observations.[12,14,15] We compare our estimates with coal mine

Received: June 16, 2021
Revised: October 25, 2021
Accepted: October 26, 2021
Published: November 29, 2021

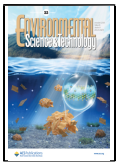

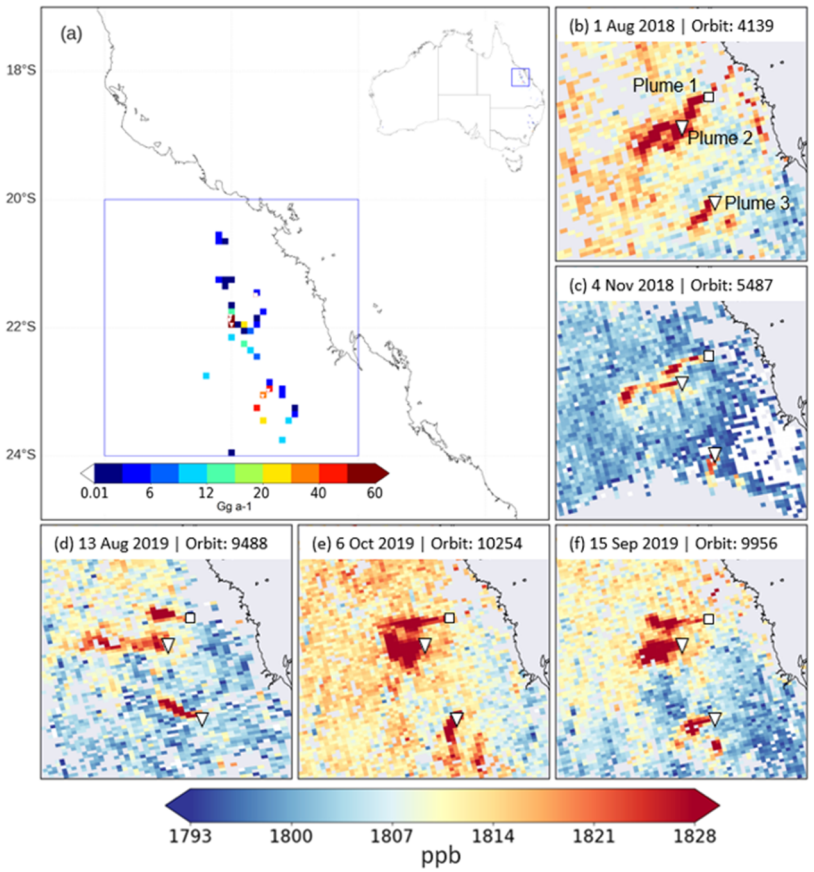

Figure 1. TROPOMI observations and methane emissions over the study domain. Panel (a) shows a 0.1 × 0.1° gridded map of reconstructed bottom-up methane emissions from coal mines in Queensland, Australia (19). The blue square ranging from latitude 20°−24°S and longitude 146°−150°E indicates the domain containing the three source locations of our study. The inset panel shows the map of Australia and the relative location of the study domain, which lies in the northeast. Examples of the persistent XCH_4 plumes observed are shown for different TROPOMI orbits over the study domain (b−f) during 2018 and 2019. The surface mine at source 1 is identified by the square at the origin of the top plume, and the underground mines at sources 2 and 3 are indicated with triangles near the middle and the bottom plumes. Cloud-free observations are mostly found during the months of June until November in both years. TROPOMI methane column (XCH_4) is given in ppb, and the gridded methane emissions inside the study domain are given in Gg a^{-1}.

emissions from a global inventory and those officially reported by Australia to the United Nations Framework Convention on Climate Change (UNFCCC).[18] The study highlights the superemitter behavior of three coal mines or coal mine clusters. The identification and quantification of integrated overall methane fluxes from coal production sites using satellite observations can help to further improve the national inventory and prioritize emission reduction targets.

MATERIALS AND METHODS

TROPOMI Observations. The TROPOMI scientific data product used here was retrieved using the RemoTeC full-physics algorithm with improvements that resulted in a more stable retrieval and correction for surface albedo biases.[20] Total column methane (XCH_4) is retrieved with nearly uniform sensitivity in the troposphere from its absorption band around 2.3 and 0.7 μm using earthshine radiance measurements from the shortwave infrared (SWIR) and near-infrared (NIR) channel of TROPOMI.[20−22] This new dataset has shown good agreement with the measurements from the well-established Total Carbon Column Observing Network (TCCON)[23] and with the Greenhouse gases Observing SATellite−GOSAT.[24] The TROPOMI XCH_4 measurements used in this analysis were screened for cloud-free coverage and low aerosol content using the quality flag provided in the data products (we use qa = 1). Data quality qa = 1 signifies XCH_4 is filtered for solar zenith angle (<70°), viewing zenith angle (<60°), smooth topography (1 standard deviation surface elevation variability <80 m within a 5 km radius), and low aerosol load (aerosol optical thickness <0.3 in the NIR band). The TROPOMI data was corrected for XCH_4 variations due to surface elevation by adding 7 ppb per km surface elevation with respect to the mean sea level.[25] TROPOMI XCH_4 data show artificial stripes in the flight direction, most probably due to swath position-dependent calibration inaccuracies, which were corrected by applying a fixed mask destriping approach to the L2 data developed for the TROPOMI XCO retrieval.[26,27]

For emission quantification from TROPOMI-detected plumes, orbits from 2018 and 2019 were screened with >500 individual observation pixels in the domain of 20°−24°S and 146°−150°E (Figure 1a). To ensure that emission quantifications are not influenced by systematic surface albedo or aerosol bias, we reject orbits that show a high correlation ($|R| > 0.5$) of XCH_4 with surface albedo or aerosol optical thickness. Seventy-five orbits containing a total of 124 clear-sky observations over the three sources were thus selected and used for emission quantification. The temporal spread shows most observations in the months of July−December in both 2018 and 2019 (Figure

https://doi.org/10.1021/acs.est.1c03976
Environ. Sci. Technol. 2021, 55, 16573−16580

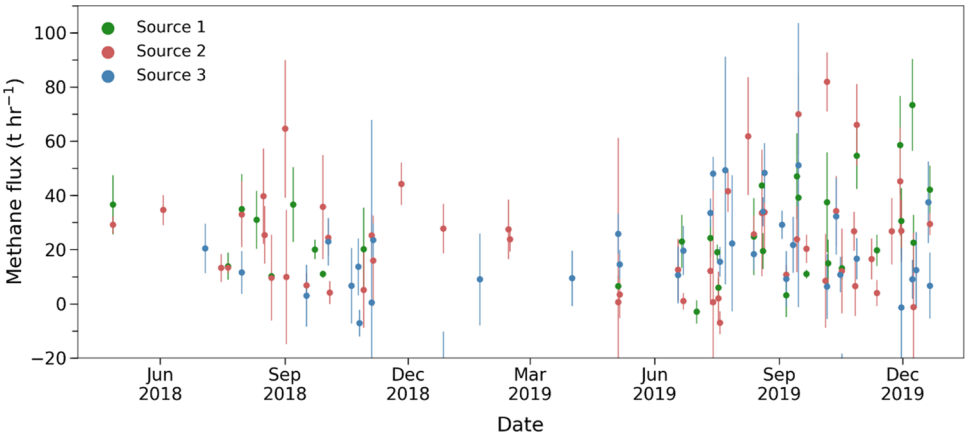

Figure 2. Methane emission fluxes quantified from individual TROPOMI observations. Daily methane flux estimates derived from TROPOMI observations for the three sources that were used for the annual quantification. A total of 124 clear-sky scenes spanning over the source areas from 75 orbits are shown here. The methane source rate for each XCH_4 plume is given with its uncertainty (1σ).

2). The presence of clouds during January until June limits the availability of TROPOMI during these months. However, quarterly raw coal production numbers in 2018 and 2019 show variations of less than 5%, so we expect only minor differences in emission rates over the year.

Cross-Sectional Flux Method. We quantify methane emissions from TROPOMI observations using the cross-sectional flux method,[28] as shown in eq 1.

$$Q = \overline{C}U_{\text{eff}} \text{ where, } \overline{C} = \frac{1}{n} \times \sum_{j=1}^{n} \int \Delta\Omega(x_j, y)\mathrm{d}y \quad (1)$$

where the source rate Q (t h^{-1}) is calculated as the product of the integrated methane column enhancement $\overline{C}$ and the effective wind speed U_{eff}. The methane column enhancement $\Delta\Omega$ (x_j, y) is computed by sampling the plume using transects orthogonal to the plume direction (y-axis) in the downwind of the source (x-axis) (Figure S1). The sampled observations are integrated across each transect within limits defined by the length of the transect. For a daily source rate, we take the mean of all of the emission estimates calculated for individual transects ($j = 1,..., n$, where n is the number of transects) between the source and the end of the plume. For deriving the effective wind speed (U_{eff}), we use the pressure-weighted average boundary layer wind speed U_{blh} from ERA5 meteorology. Varon et al.[14] derived a relationship between U_{eff} and U_{blh} for TROPOMI observations as $U_{\text{eff}} = (1.05 \pm 0.17)\ U_{\text{blh}}$ using the Weather Research and Forecasting model coupled with chemistry (WRF-Chem), where modeled methane emissions were compared with the cross-sectional flux estimates. For our case, we have assumed $U_{\text{eff}} = U_{\text{blh}}$.

Transects across the plume have been defined for each source by estimating the downwind direction and dimensions of the plume. We start with a smaller rectangular mask of dimension (length × breadth) 0.4 × 0.2° placed at the source in the downwind direction inferred from boundary layer average ERA5 meteorology to define the area containing the plume (Figure S1). Next, we rotate this mask from −40 to +40° at 5° intervals around the inferred ERA5 wind direction such that the average XCH_4 enhancement in the rectangular mask is maximal. After we set the new wind direction, the length of the rectangular mask in the downwind direction (along the x-axis) is varied to define the end of the plume. This end is fixed by incrementing the length of the rectangular mask by 0.1° intervals until the difference between methane enhancement of two consecutive increments is less than 5 ppb. Similarly, the width of the rectangular mask (along the y-axis) was fixed by incrementing the width in the lateral direction of the plume at an interval of 0.05° until the incremental change in methane enhancement is less than 5 ppb.

We define 15 equally spaced transects between the source and the end of the rectangular mask for calculating the source rates. We ignore the first three transects due to their close proximity to the source, where XCH_4 may be underestimated due to partial pixel enhancement.[12,14] To avoid underestimation of emissions due to incomplete sampling of the plume by a transect due to missing pixels, we only consider transects that have more than 75% overlap with TROPOMI pixels. With this requirement, we only calculate the source rate from plumes with at least three or more transects. The methane enhancement for each pixel along the transects is defined relative to the background XCH_4, which is calculated as the average of 0.5 × 0.5° area centered at a distance of 0.1° upwind from the source. If the number of background observations is less than 20, we use the median XCH_4 of all pixels in the domain (20°−24°S, 146°−150°E) as background XCH_4. To account for other emissions in the downwind plume, we subtract the contributions from surrounding coal mines[18,19] (Figure S2b), the other anthropogenic sources from EDGARv4.3.2 global emissions[5] (Figure S3b) and emissions from oil and gas[29] (Figure S3c) within the plume for each source. In some cases, we estimate small negative emissions as shown in Figure 2, possibly due to high XCH_4 values in the background. As the location of the background and source regions are shifting around the source with changes in daily wind directions, we expect this error to average out in the mean source rate. We compute the uncertainty in the daily emission rate by accounting for the uncertainty in the mean enhancement, the pressure-weighted average boundary layer ERA5 wind speed, and the uncertainty derived from U_{eff} and U_{blh} equation (see Supporting Information, Section S1).

Bottom-Up Emission Estimates. The bottom-up emissions from the global inventory of EDGARv4.3.2[5] (most recent year 2012) and the Australian national inventory reporting[30] (for 2018) were used in this study to compare with the TROPOMI emission estimates. EDGARv4.3.2 uses tier-1 (global default emission factors) and some tier-2 (region-specific) information to estimate national emissions from all anthropogenic sources. These emissions are available on a 0.1 ×

https://doi.org/10.1021/acs.est.1c03976
Environ. Sci. Technol. 2021, 55, 16573−16580

Table 1. Source Location Details and Methane Emission Quantification Using TROPOMI Observations

details	source 1	source 2	source 3
location	Hail Creek	Broadmeadow, Moranbah North, and Grosvenor	Grasstree and Oaky North
mine type	surface	underground	underground
mining method	Dragline, truck and shovel	longwall	longwall
total raw coal production in million tonnes	2018−19: 7.7	2018−19: 19.2[a]	2018−19: 13.7[b]
	2019−20: 5.8	2019−20: 19.0[a]	2019−20: 12.4[b]
longitude, latitude	148.380°E, 21.490°S	147.980°E, 21.825°S	148.579°E, 22.988°S 148.486°E, 23.072°S
		147.967°E, 21.885°S	
		147.996°E, 21.962°S	
number of clear-sky observations in TROPOMI	32	54	38
annual emissions using the CSF method (Gg a^{-1}) [$\mu \pm 2\sigma$]	230 ± 50	190 ± 60	150 ± 63

[a]Includes raw coal production from Broadmeadow, Moranbah North, and Grosvenor underground coal mines. [b]Includes raw coal production from Grasstree and Oaky North underground coal mines.

0.1° grid, allowing comparison with the observations. For this purpose, the 2012 EDGAR emissions from coal mines were scaled to 2018 using the ratio in coal production from 2012 to 2018 of Queensland state (the derived 2018 emissions are referred to as EDGARv4.3.2*). As the location of EDGAR emissions for coal mines does not exactly match the locations of the sources studied here, the emissions in the grid cell closest to the source locations were chosen as representing these coal mine locations (Figure S3a). The Australian national inventory report (NIR) utilizes more detailed tier-2 and tier-3 (facility-specific) methodologies but is not available at a resolution beyond the state level. The national inventory provides methane emissions from coal for the categories of surface mines and underground mines at the state level.[30] For the emissions associated with the coal mines of study, we use gridded emissions from Sadavarte et al.[19] These emissions were estimated using grouped emissions in the surface and underground category at the state level from the national inventory and distributed these to the respective surface and underground coal mines within the state using coal production of individual mines as a distribution proxy along with the gas content profiles of the coal basins.[19] Section S2 of the supporting information provides the link to access the data used in the analyses.

RESULTS AND DISCUSSION

TROPOMI Localization of Emission Sources. For the three distinct plumes that are consistently visible in the TROPOMI methane data over the Bowen Basin in Queensland state, we use the wind-rotation technique described by Maasakkers et al.[31] combined with the reconstructed high-resolution bottom-up inventory by Sadavarte et al.[19] (Figure S2) to determine which sources are responsible for the enhancements. The wind-rotation method (see Supporting Information, Section S3) traces the location of a source by averaging TROPOMI data after aligning the observations from individual days with the local wind vector (from GEOS-FP 10 m).[32] The source location is then determined by comparing the resulting averaged rotated downwind "plumes" for a full grid of rotation points. For the most northern plume seen in TROPOMI, we identify the emission source to be the Hail Creek surface mine. The middle plume originates from the underground mines of Broadmeadow, Moranbah North, and Grosvenor, and for the most southern plume, the Grasstree and Oaky North underground mines are responsible (see Supporting Information, Section S3). Given the limited spatial resolution of the TROPOMI observations and the close vicinity of the coal mines at the second and third source locations, we could not further distinguish the contributions of the individual mines. Table 1 summarizes the details about the geographical location, mining type, and production. Supporting Information, Figure S4 shows the satellite imagery of the source locations.

TROPOMI Methane Emission Quantification and Uncertainty Estimate. For the emission quantification, we screen individual TROPOMI orbits for sufficient spatial coverage over the region (20°−24°S and 146°−150°E), source locations, data-quality indicators, and favorable wind speed conditions. Figure 1 shows a few typical observations with signals from the three source locations clearly visible in the data. For each selected orbit, methane emissions are quantified for each source location using the cross-sectional flux method.[28] In this method, emissions are calculated by taking the product of line integrals of methane enhancements and wind speed, perpendicular to the downwind direction of the methane plume, similar to Varon et al.[14] A total of 124 plumes from 75 screened orbits have been quantified for the period 2018−2019 (Figure 2). We use the average boundary layer ERA5 wind speed for the TROPOMI overpass time of 04:00 UTC. Figure 2 shows the temporal variability in the methane flux from the three source locations with the uncertainty of one standard deviation on each source rate. We estimate relative uncertainties of 55% on average (range of 18−98%) on the daily emission source rates for non-negative enhancements. These uncertainties include the standard deviation in the different transects used in the CSF; the uncertainty in the background by varying the area it is calculated over; and the uncertainty in the wind speed using wind speeds within ± 2 h of the overpass time (see Supporting Information, Section S1). The largest uncertainties are caused by the presence of high methane in the background, making it difficult to isolate the mine's signal and cases with low wind speeds as influences from turbulent transport become important, which are not accounted for in our method.[28] Therefore, estimates at wind speeds below 2 m s^{-1} are excluded. The number of days with emission quantifications is mainly limited by the presence of cloud cover but although there is quite some variation in the daily estimates and the error on each methane flux, the number of observations in combination with the random sampling over a 2 year period is representative of the methane source and sufficient to quantify annual emissions.[15]

The combined annual methane emission from the three persistent (more than 75% of the 124 screened orbits had high

https://doi.org/10.1021/acs.est.1c03976
Environ. Sci. Technol. 2021, 55, 16573−16580

methane enhancements downwind of the source locations) sources is estimated at 570 ± 98 Gg a^{-1} (Figure 3). Multiple

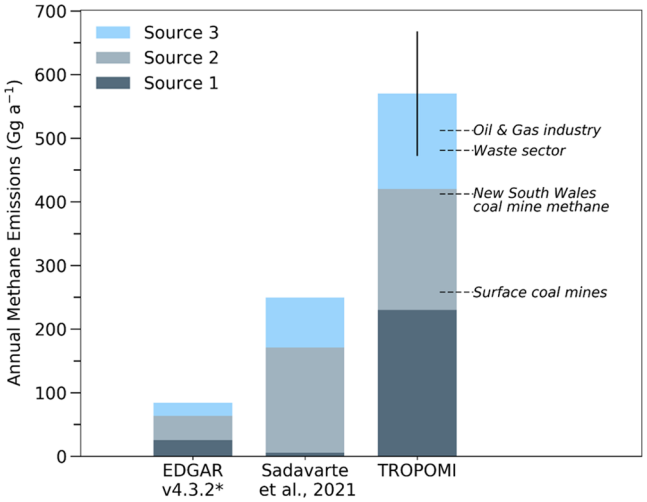

Figure 3. Annual methane emissions for three coal mine sources. Annual methane emission estimates for the coal mine sources of the persistent plumes observed in TROPOMI data. The left bar shows the annual methane emissions from the global inventory of EDGARv4.3.2 available for 2012. EDGARv4.3.2* indicates the projected emissions for 2018 calculated after accounting for the change in coal production in Queensland state in 2018 relative to 2012. The middle bar shows the reconstructed bottom-up emissions from Sadavarte et al.[19] for the three sources using national emissions communicated to UNFCCC for 2018 and proxies such as coal production for individual mines and the gas content profile. The right bar shows the total annual emissions estimated using TROPOMI observations for the period 2018−2019. The error bar represents 2σ uncertainty (95% confidence interval). Total emissions from TROPOMI are also compared with nationally reported greenhouse gas emissions from selected sectors and categories of Australia for 2018 using the dashed horizontal lines on the TROPOMI bar.

sensitivity tests confirm the robustness of our emission estimate within its uncertainty (see Supporting Information, Section S1, Figure S5, Table S1). Together, the three sources emit a factor of 7 more than their bottom-up estimates in the global EDGARv4.3.2* emission inventory (84 Gg a^{-1}).[5] Our estimate is also higher by a factor of 2 compared to the reconstructed high-resolution bottom-up (RBU) emissions from the national inventory report (250 Gg a^{-1})[18,19] There is reasonable agreement between the national methane emission from coal mines reported by EDGARv4.3.2 (1228 Gg a^{-1} for 2012) and the national inventory report for 2018 (972 Gg a^{-1}). The large difference in emissions between the three sources in these two inventories (Figure 3) is most likely explained by the different spatial proxies used for the disaggregation of national methane emissions (Figures S2b and S3a). The EDGARv4.3.2 global inventory[5] uses coal production activity from the World Coal Association and spatial proxies from the Global Energy Observatory for all countries other than the United States (USGS coal mines), Europe (EPRTRv4.2), and China[33] while the Sadavarte et al.[19]−inventory uses Australian UNFCCC NIR reported emissions at the state level and spatially distributes these emissions using coal mine locations from the Queensland state web portal.[34] In short, EDGAR distributes the emissions over a much larger number of locations, and it is not surprising that for the individual locations, a discrepancy is found. Since the coal mine locations of the Queensland state web portal were also verified from the mining operation reports of coal mine companies, we believe these locations to be the most reliable.

Focusing on the individual sources, our estimate for Hail Creek is more than 35 times the reconstructed bottom-up emission[19] (RBU: 6 Gg a^{-1}, TROPOMI: 230 ± 50 Gg a^{-1}) and 15% higher than the reported methane emission from all surface mines in Queensland state combined (196 Gg a^{-1}) (Table S2). Our Hail Creek estimate accounts for 88% of Australia's total reported surface coal mine emissions, suggesting a large underreporting of methane emissions in the national inventory reporting for surface mines (Figure 3, Table S3). Similarly, emissions from Grasstree and Oaky North underground mines are a factor of 2 higher[19] (RBU—79 Gg a^{-1}, TROPOMI—150 ± 63 Gg a^{-1}), while emissions from the Broadmeadow, Moranbah North, and Grosvenor mines are consistent with the reconstructed estimate[19] (RBU—165 Gg a^{-1}, TROPOMI—190 ± 60 Gg a^{-1}).

Comparing Emissions with National Estimates. Applying the cross-sectional flux method to 2 years of TROPOMI observations, we estimate a total methane source strength of 570 ± 98 Gg a^{-1} for the three source locations, equivalent to an average methane flux of 65 ± 11 t h^{-1}. This can be broken down to 230 ± 50 Gg a^{-1} CH_4 emissions from source 1 (a single surface mine) and 340 ± 86 Gg a^{-1} CH_4 from sources 2 and 3 (five underground mines). To put these emissions in the national context, we compare them to Australian methane emissions from other source sectors. Our estimate for these three coal mine sources represents over 10% of the total reported methane emission from Australia in 2018 and exceeds the emission from the oil and gas industry sector (512 Gg a^{-1}), as well as the entire waste sector (480 Gg a^{-1}) (Figure 3 and Table S3). The six mines produce only 7% of the national raw coal production (41 million tonnes) but represent 55% of the national methane emissions from coal production reported for 2018 (Tables S2 and S3). The Hail Creek mine alone emits 20% of the national CH_4 emission from coal mining while accounting for only 1% of the national coal production.

Analyzing the TROPOMI-Derived Emission Factor for Australian Coal Mines. Australia, and in particular the state of Queensland, is known for its production of liquified natural gas (LNG) by extracting coal seam gas (CSG) from the methane-rich Bowen and Surat basins, which is also being exported internationally since 2015.[35] The gassy nature of the underground mines in Queensland state is well established and allowed the infrastructure not only to release methane to the atmosphere through ventilation shafts but also to capture and utilize it for power generation or flare or transfer off-site (see Supporting Information, Section S4). Australia reports methane emissions from underground mines using a tier-3 Intergovernmental Panel on Climate Change (IPCC) accounting method, using country-specific methodologies and respective mine-specific measured emissions factors (see Supporting Information, Section S5). These tier-3 emissions are not disclosed publicly for individual mines but grouped and reported at the state level in the national inventory report[18,30] (Queensland state produced 51% of the raw coal and emitted 56% of the national fugitive methane from coal mines[18,30] (Supporting Information, Table S2)). This hampers direct verification of mine-specific emissions using atmospheric measurements, like those from TROPOMI. In the case of surface mines, methane emissions are likely unabated and escape to the atmosphere throughout the mining operations. Although, as per NGER guidelines, "venting or flaring of in situ gas can also

https://doi.org/10.1021/acs.est.1c03976
Environ. Sci. Technol. 2021, 55, 16573−16580

occur from open-cut coal mines", it is less common and less efficient since the coal seam is in direct contact with the atmosphere, providing a diffusion pathway that is difficult to capture. Moreover, the combustion of large gas volumes with a low CH_4 content is more expensive than with higher concentrations. For national inventory reporting, these emissions are calculated using a mix of tier-2/tier-3 emission factors and coal production data.[30] The tier-3 emission factors in Australia are measured following the National Greenhouse and Energy Report guidelines[36] for each surface mine in the Gunnedah, Western, Surat, Collie, Hunter, and Newcastle basins only. The surface mines in the Bowen basin, including Hail Creek, use a tier-2 basin-average emission factor (1.2 m^3 CH_4/tonne of raw coal) from William et al.[37,30] It is difficult to assess how representative this tier-2 approach is for the local situation, but our results indicate that it leads to a severe underestimation in the case of Hail Creek.

The emission factor inferred from TROPOMI data for the underground mines 2 and 3 amounts to 10−11.50 g CH_4 per kg raw coal, consistent with emission factors from EDGARv4.3.2, IPCC default values, and Kholod et al.[6] for mining at 200−400 m depth (Table S4), whereas the national and state-level emission factors for underground mines (for 2017 and 2018) are 25−50% lower than TROPOMI-based implied emission factor (Table S4). Lower country-specific emission factors compared to IPCC defaults in itself are not surprising as local coal type and mitigation measures play an important role, but we notice that especially for the mines of source 3, they are not in line with the TROPOMI-based observations. For surface mine Hail Creek (source 1), the TROPOMI-inferred emission factor is 34 g CH_4 per kg raw coal, 22 times higher than the average of the IPCC default for <200 m and Kholod et al.,[6] i.e., 0.2, 0.52, and 2.03−3.38 g CH_4 per kg raw coal (Table S4).

Understanding the Superemitting Behavior of Hail Creek. The Hail Creek mine was approved for an extension to highwall and underground mining activities in 2016.[38] Sentinel-2 satellite images over Hail Creek for 2018 to 2019 do not, however, show any significant change to the Northeast of the surface mine, where the extension was proposed (see Supporting Information, Movie S1). The preparatory activities are seen to the Northeast of the surface mine, suggesting possible premining degasification, starting before 2018. Typically, the degasification or predrainage is performed prior to underground mining as a safety measure against outbursts in the underground mine (see Supporting Information, Section S4). It involves draining the seam gas by either natural or active venting, combusting and/or flaring on-site or transferring off-site.[36] We do observe flaring activities over the extended area in July−September 2019[39] (Figure S6). However, no flaring activity was observed for the remainder of the analysis period in 2018−2019.[39] Most likely, the TROPOMI-detected emissions at Hail Creek in 2018 and 2019 are due to surface mining and also possibly from predrainage activities.

In conclusion, to reduce the uncertainty in methane leakage from fossil fuel production, it is crucial to have accurate estimates of methane emissions from coal production. The TROPOMI instrument does not have the granularity of the ground-based measurements and/or monitoring of individual shafts as done by the mining companies. However, its observations provide a useful measure of emissions from the entire coal mine infrastructure, including emissions from ventilation shafts and other pre- and post-drainage systems like underground in-seam (UIS), surface to in-seam (SIS), and gas wells drilled for underground mines and any other unforeseen leakage. The good agreement for source 2 with the reconstructed bottom-up emissions shows that there can be a good agreement with bottom-up reporting. When applying exactly the same method and approach to source 3 and source 1, however, we find large discrepancies with the reported values. The TROPOMI-inferred emission factor for source 3 (underground mines) is consistent with global studies and also with the value derived for source 2. On the other hand, for source 1 (surface mine Hail Creek), we find unexpected high emission for a surface coal mine and an implied emission factor that is more than an order of magnitude higher than any default factor in current IPCC guidelines for this source type. Overall, we find higher amounts of methane emitted, especially from the Hail Creek surface mine, pointing to the underreporting of Australian methane emissions to a level that would justify a revision of the national methane emission reported in the NIR to the UNFCCC. Our results show that satellite observations can provide a measurement-based integral quantification of an entire facility or production site. This is valuable complementary information next to emission estimates of individual processes or mine shafts. It can help to further improve national emission inventories and support the identification of the most promising targets for mitigation.

■ ASSOCIATED CONTENT

Supporting Information

The Supporting Information is available free of charge at https://pubs.acs.org/doi/10.1021/acs.est.1c03976.

Sections on uncertainty estimate for each source rate, plume rotation method, and methane emissions reporting of underground coal mines in Australia along with supporting tables and figures (PDF)

Supporting animation of Sentinel-2 satellite imagery over Hail Creek coal mine (Movie S1) (AVI)

■ AUTHOR INFORMATION

Corresponding Author

Pankaj Sadavarte − *SRON Netherlands Institute for Space Research, 3584 CA Utrecht, The Netherlands; Department of Climate, Air and Sustainability, TNO, 3584 CB Utrecht, The Netherlands;* orcid.org/0000-0002-7337-683X; Email: p.sadavarte@sron.nl

Authors

Sudhanshu Pandey − *SRON Netherlands Institute for Space Research, 3584 CA Utrecht, The Netherlands*

Joannes D. Maasakkers − *SRON Netherlands Institute for Space Research, 3584 CA Utrecht, The Netherlands;* orcid.org/0000-0001-8118-0311

Alba Lorente − *SRON Netherlands Institute for Space Research, 3584 CA Utrecht, The Netherlands*

Tobias Borsdorff − *SRON Netherlands Institute for Space Research, 3584 CA Utrecht, The Netherlands*

Hugo Denier van der Gon − *Department of Climate, Air and Sustainability, TNO, 3584 CB Utrecht, The Netherlands*

Sander Houweling − *SRON Netherlands Institute for Space Research, 3584 CA Utrecht, The Netherlands; Department of Earth Sciences, Vrije Universiteit, Amsterdam, 1081 HV Amsterdam, The Netherlands*

Ilse Aben − *SRON Netherlands Institute for Space Research, 3584 CA Utrecht, The Netherlands*

https://doi.org/10.1021/acs.est.1c03976
Environ. Sci. Technol. 2021, 55, 16573−16580

Complete contact information is available at:
https://pubs.acs.org/10.1021/acs.est.1c03976

Author Contributions

P.S. and S.P. analyzed the TROPOMI data, performed the mass balance calculation and sensitivity studies with inputs from S.H. and I.A.; J.D.M. performed localization method for identification of coal mines; A.L. processed the operational data product of TROPOMI methane for 2018 and 2019; T.B. provided the support for de-stripping of TROPOMI orbits; P.S. and H.D.v.d.G. contributed to the bottom-up inventory analysis. P.S. wrote the manuscript with inputs from all of the co-authors.

Funding

This work was supported through the GALES project (#15597) by the Dutch Technology Foundation STW, and the TROPOMI national program through NSO. P.S. and S.P. are funded through the GALES project (#15597) by the Dutch Technology Foundation STW, which is part of the Netherlands Organization for Scientific Research (NWO). A.L. and T.B. acknowledge funding from the TROPOMI national program through NSO.

Notes

The authors declare no competing financial interest.

■ ACKNOWLEDGMENTS

The authors thank the Earth Science Group team at SRON for developing the retrieval method for TROPOMI methane observation and consistent technical support throughout the period. The authors thank the team that realized the TROPOMI instrument and its data products consisting of the partnership between Airbus Defense and Space Netherlands, KNMI, SRON, and TNO, commissioned by NSO and ESA. Sentinel-5 Precursor is part of the EU Copernicus program, and Copernicus Sentinel data of Scientific version for 2018−2019 have been used. The authors thank Prof. Bryce Kelly, University of New South Wales, for his continuous support and expert knowledge on coal mines in Australia. The authors acknowledge the provision of publicly available global bottom-up emission of greenhouse gases from EDGAR and the meteorology data product of ERA5.

■ REFERENCES

(1) Myhre, G.; Shindell, D.; Bréon, F. M.; Collins, W.; Fuglestvedt, J.; Huang, J.; Koch, D.; Lamarque, J. F.; Lee, D.; Mendoza, B.; Nakajima, T.; Robock, A.; Stephens, G.; Takemura, T.; Zhang, H. Anthropogenic and Natural Radiative Forcing. In *Climate Change 2013: The Physical Science Basis. Contribution of Working Group I to the Fifth Assessment Report of the Intergovernmental Panel on Climate Change (IPCC)*; Stocker, T. F.; Qin, D.; Plattner, G.-K.; Tignor, M.; Allen, S. K.; Boschung, J.; Nuales, A.; Xia, Y.; Bex, V.; Midgley, P. M., Eds.; Cambridge University Press: Cambridge, UK and New York, 2013; pp 659−740.

(2) Shindell, D.; Kuylenstierna, J. C. I.; Vignati, E.; van Dingenen, R.; Amann, M.; Klimont, Z.; Anenberg, S. C.; Muller, N.; Janssens-Maenhout, G.; Raes, F.; Schwartz, J.; Faluvegi, G.; Pozzoli, L.; Kupiainen, K.; Höglund-Isaksson, L.; Emberson, L.; Streets, D.; Ramanathan, V.; Hicks, K.; Oanh, N. T. K.; Milly, G.; Williams, M.; Demkine, V.; Fowler, D. Simultaneously mitigating near-term climate change and improving human health and food security. *Science* **2012**, *335*, 183−189.

(3) Nisbet, E. G.; Manning, M. R.; Dlugokencky, E. J.; Fisher, R. E.; Lowry, D.; Michel, S. E.; Lund Myhre, C.; Platt, S. M.; Allen, G.; Bousquet, P.; Brownlow, R.; Cain, M.; France, J. L.; Hermansen, O.; Hossaini, R.; Jones, A. E.; Levin, I.; Manning, A. C.; Myhre, G.; Pyle, J. A.; Vaughn, B. H.; Warwick, N. J.; White, J. W. C. Very strong atmospheric methane growth in the 4 years 2014−2017: Implications for the Paris Agreement. *Global Biogeochem. Cycles* **2019**, *33*, 318−342.

(4) Saunois, M.; Stavert, A. R.; Poulter, B.; Bousquet, P.; Canadell, J. G.; Jackson, R. B.; Raymond, P. A.; Dlugokencky, E. J.; Houweling, S.; Patra, P. K.; Ciais, P.; Arora, V. K.; Bastviken, D.; Bergamaschi, P.; Blake, D. R.; Brailsford, G.; Bruhwiler, L.; Carlson, K. M.; Carrol, M.; Castaldi, S.; Chandra, N.; Crevoisier, C.; Crill, P. M.; Covey, K.; Curry, C. L.; Etiope, G.; Frankenberg, C.; Gedney, N.; Hegglin, M. I.; Höglund-Isaksson, L.; Hugelius, G.; Ishizawa, M.; Ito, A.; Janssens-Maenhout, G.; Jensen, K. M.; Joos, F.; Kleinen, T.; Krummel, P. B.; Langenfelds, R. L.; Laruelle, G. G.; Liu, L.; Machida, T.; Maksyutov, S.; McDonald, K. C.; McNorton, J.; Miller, P. A.; Melton, J. R.; Morino, I.; Müller, J.; Murguia-Flores, F.; Naik, V.; Niwa, Y.; Noce, S.; O'Doherty, S.; Parker, R. J.; Peng, C.; Peng, S.; Peters, G. P.; Prigent, C.; Prinn, R.; Ramonet, M.; Regnier, P.; Riley, W. J.; Rosentreter, J. A.; Segers, A.; Simpson, I. J.; Shi, H.; Smith, S. J.; Steele, L. P.; Thornton, B. F.; Tian, H.; Tohjima, Y.; Tubiello, F. N.; Tsuruta, A.; Viovy, N.; Voulgarakis, A.; Weber, T. S.; van Weele, M.; van der Werf, G. R.; Weiss, R. F.; Worthy, D.; Wunch, D.; Yin, Y.; Yoshida, Y.; Zhang, W.; Zhang, Z.; Zhao, Y.; Zheng, B.; Zhu, Q.; Zhu, Q.; Zhuang, Q. The Global Methane Budget 2000−2017. *Earth Syst. Sci. Data* **2020**, *12*, 1561−1623.

(5) Janssens-Maenhout, G.; Crippa, M.; Guizzardi, D.; Muntean, M.; Schaaf, E.; Dentener, F.; Bergamaschi, P.; Pagliari, V.; Olivier, J. G. J.; Peters, H. W.; van Aardenne, J. A.; Monni, S.; Doering, U.; Petrescu, A. M. R.; Solazzo, E.; Oreggioni, G. D. EDGAR v4.3.2 Global Atlas of the three major greenhouse gas emissions for the period 1970−2012. *Earth Syst. Sci. Data* **2019**, *11*, 959−1002.

(6) Kholod, N.; Evans, M.; Pilcher, R. C.; Roshchanka, V.; Ruiz, F.; Coté, M.; Collings, R. Global methane emissions from coal mining to continue growing even with declining coal production. *J. Cleaner Prod.* **2020**, *256*, No. 120489.

(7) Saunois, M.; Bousquet, P.; Poulter, B.; Peregon, A.; Ciais, P.; Canadell, J. G.; Dlugokencky, E. J.; Etiope, G.; Bastviken, D.; Houweling, S.; Janssens-Maenhout, G.; Tubiello, F. N.; Castaldi, S.; Jackson, R. B.; Alexe, M.; Arora, V. K.; Beerling, D. J.; Bergamaschi, P.; Blake, D. R.; Brailsford, G.; Brovkin, V.; Bruhwiler, L.; Crevoisier, C.; Crill, P.; Covey, K.; Curry, C.; Frankenberg, C.; Gedney, N.; Höglund-Isaksson, L.; Ishizawa, M.; Ito, A.; Joos, F.; Kim, H.-S.; Kleinen, T.; Krummel, P.; Lamarque, J.-F.; Langenfelds, R.; Locatelli, R.; Machida, T.; Maksyutov, S.; McDonald, K. C.; Marshall, J.; Melton, J. R.; Morino, I.; Naik, V.; O'Doherty, S.; Parmentier, F.-J. W.; Patra, P. K.; Peng, C.; Peng, S.; Peters, G. P.; Pison, I.; Prigent, C.; Prinn, R.; Ramonet, M.; Riley, W. J.; Saito, M.; Santini, M.; Schroeder, R.; Simpson, I. J.; Spahni, R.; Steele, P.; Takizawa, A.; Thornton, B. F.; Tian, H.; Tohjima, Y.; Viovy, N.; Voulgarakis, A.; van Weele, M.; van der Werf, G. R.; Weiss, R.; Wiedinmyer, C.; Wilton, D. J.; Wiltshire, A.; Worthy, D.; Wunch, D.; Xu, X.; Yoshida, Y.; Zhang, B.; Zhang, Z.; Zhu, Q. The Global Methane Budget 2000−2012. *Earth Syst. Sci. Data* **2016**, *8*, 697−751.

(8) Krings, T.; Gerilowski, K.; Buchwitz, M.; Hartmann, J.; Sachs, T.; Erzinger, J.; Burrows, J. P.; Bovensmann, H. Quantification of methane emission rates from coal mine ventilation shafts using airborne remote sensing data. *Atmos. Meas. Tech.* **2013**, *6*, 151−166.

(9) Luther, A.; Kleinschek, R.; Scheidweiler, L.; Defratyka, S.; Stanisavljevic, M.; Forstmaier, A.; Dandocsi, A.; Wolff, S.; Dubravica, D.; Wildmann, N.; Kostinek, J.; Jöckel, P.; Nickl, A.-L.; Klausner, T.; Hase, F.; Frey, M.; Chen, J.; Dietrich, F.; Nęcki, J.; Swolkień, J.; Fix, A.; Roiger, A.; Butz, A. Quantifying CH4 emissions from hard coal mines using mobile sun-viewing Fourier transform spectrometry. *Atmos. Meas. Tech.* **2019**, *12*, 5217−5230.

(10) Kort, E. A.; Frankenberg, C.; Costigan, K. R.; Lindenmaier, R.; Dubey, M. K.; Wunch, D. Four corners: The largest US methane anomaly viewed from space. *Geophys. Res. Lett.* **2014**, *41*, 6898−6903.

(11) Turner, A. J.; Jacob, D. J.; Wecht, K. J.; Maasakkers, J. D.; Lundgren, E.; Andrews, A. E.; Biraud, S. C.; Boesch, H.; Bowman, K. W.; Deutscher, N. M.; Dubey, M. K.; Griffith, D. W. T.; Hase, F.; Kuze, A.; Notholt, J.; Ohyama, H.; Parker, R.; Payne, V. H.; Sussmann, R.; Sweeney, C.; Velazco, V. A.; Warneke, T.; Wennberg, P. O.; Wunch, D. Estimating global and North American methane emissions with high

spatial resolution using GOSAT satellite data. *Atmos. Chem. Phys.* **2015**, *15*, 7049−7069.
(12) Pandey, S.; Gautam, R.; Houweling, S.; van der Gon, H. D.; Sadavarte, P.; Borsdorff, T.; Hasekamp, O.; Landgraf, J.; Tol, P.; van Kempen, T.; Hoogeveen, R.; van Hees, R.; Hamburg, S. P.; Maasakkers, J. D.; Aben, I. Satellite observations reveal extreme methane leakage from a natural gas well blowout. *Proc. Natl. Acad. Sci. U.S.A.* **2019**, *116*, 26376−26381.
(13) Zhang, Y.; Gautam, R.; Pandey, S.; Omara, M.; Maasakkers, J. D.; Sadavarte, P.; Lyon, D.; Nesser, H.; Sulprizio, M. P.; Varon, D. J.; Zhang, R.; Houweling, S.; Zavala-Araiza, D.; Alvarez, R. A.; Lorente, A.; Hamburg, S. P.; Aben, I.; Jacob, D. J. Quantifying methane emissions from the largest oil-producing basin in the United States from space. *Sci. Adv.* **2020**, *6*, No. eaaz5120.
(14) Varon, D. J.; McKeever, J.; Jervis, D.; Maasakkers, J. D.; Pandey, S.; Houweling, S.; Aben, I.; Scarpelli, T.; Jacob, D. J. Satellite discovery of anomalously large methane point sources from oil/gas production. *Geophys. Res. Lett.* **2019**, *46*, 13507−13516.
(15) Varon, D. J.; Jacob, D. J.; Jervis, D.; McKeever, J. Quantifying Time-Averaged Methane Emissions from Individual Coal Mine Vents with GHGSat-D Satellite Observations. *Environ. Sci. Technol.* **2020**, *54*, 10246−10253.
(16) Veefkind, J. P.; Aben, I.; McMullan, K.; Förster, H.; de Vries, J.; Otter, G.; Claas, J.; Eskes, H. J.; de Haan, J. F.; Kleipool, Q.; van Weele, M.; Hasekamp, O.; Hoogeveen, R.; Landgraf, J.; Snel, R.; Tol, P.; Ingmann, P.; Voors, R.; Kruizinga, B.; Vink, R.; Visser, H.; Levelt, P. F. TROPOMI on the ESA Sentinel-5 Precursor: A GMES mission for global observations of the atmospheric composition for climate, air quality and ozone layer applications. *Remote Sens. Environ.* **2012**, *120*, 70−83.
(17) Cusworth, D. H.; Jacob, D. J.; Sheng, J.-X.; Benmergui, J.; Turner, A. J.; Brandman, J.; White, L.; Randles, C. A. Detecting high-emitting methane sources in oil/gas fields using satellite observations. *Atmos. Chem. Phys.* **2018**, *18*, 16885−16896.
(18) Australian Greenhouse Emissions Information System (AGEIS). National Greenhouse Gas Inventory—UNFCCC classifications, Department of Industry, Science, Energy and Resources. https://ageis.climatechange.gov.au/ (accessed December 15, 2020).
(19) Sadavarte, P.; Pandey, S.; van der Gon, H. D.; Maasakkers, J. D.; Houweling, S.; Aben, I. A High-Resolution Gridded Inventory of Coal Mine Methane Emissions for India and Australia (2021) Submitted to Elementa: Science of the Anthropocene, 2021. https://arxiv.org/abs/2107.10317.
(20) Lorente, A.; Borsdorff, T.; Butz, A.; Hasekamp, O.; aan de Brugh, J.; Schneider, A.; Hase, F.; Kivi, R.; Wunch, D.; Pollard, D. F.; Shiomi, K.; Deutscher, N. M.; Velazco, V. A.; Roehl, C. M.; Wennberg, P. O.; Warneke, T.; Landgraf, J.; et al. Methane retrieved from TROPOMI: improvement of the data product and validation of the first two years of measurements. *Atmos. Meas. Tech.* **2021**, *14*, 665−684.
(21) Hu, H.; Hasekamp, O.; Butz, A.; Galli, A.; Landgraf, J.; Aan de Brugh, J.; Borsdorff, T.; Scheepmaker, R.; Aben, I. The operational methane retrieval algorithm for TROPOMI. *Atmos. Meas. Tech.* **2016**, *9*, 5423−5440.
(22) Hu, H.; Landgraf, J.; Detmers, R.; Borsdorff, T.; aan de Brugh, J.; Aben, I.; Butz, A.; Hasekamp, O. Toward global mapping of methane with TROPOMI: First results and intersatellite comparison to GOSAT. *Geophys. Res. Lett.* **2018**, *45*, 3682−3689.
(23) Wunch, D.; Toon, G. C.; Blavier, J.-F. L.; Washenfelder, R. A.; Notholt, J.; Connor, B. J.; Griffith, D. W. T.; Sherlock, V.; Wennberg, P. O. The Total Carbon Column Observing Network. *Philos. Trans. R. Soc., A* **2011**, *369*, 2087−2112.
(24) Kuze, A.; Suto, H.; Nakajima, M.; Hamazaki, T. Thermal and near infrared sensor for carbon observation Fourier-transform spectrometer on the Greenhouse Gases Observing Satellite for greenhouse gases monitoring. *Appl. Opt.* **2009**, *48*, 6716−6733.
(25) Buchwitz, M.; Schneising, O.; Reuter, M.; Heymann, J.; Krautwurst, S.; Bovensmann, H.; Burrows, J. P.; Boesch, H.; Parker, R. J.; Somkuti, P.; Detmers, R. G.; Hasekamp, O. P.; Aben, I.; Butz, A.; Frankenberg, C.; Turner, A. J. Satellite-derived methane hotspot emission estimates using a fast data-driven method. *Atmos. Chem. Phys.* **2017**, *17*, 5751−5774.
(26) Borsdorff, T.; aan de Brugh, J.; Pandey, S.; Hasekamp, O.; Aben, I.; Houweling, S.; Landgraf, J. Carbon monoxide air pollution on sub-city scales and along arterial roads detected by the Tropospheric Monitoring Instrument. *Atmos. Chem. Phys.* **2019**, *19*, 3579−3588.
(27) Borsdorff, T.; García Reynoso, A.; Maldonado, G.; Mar-Morales, B.; Stremme, W.; Grutter, M.; Landgraf, J. Monitoring CO emissions of the metropolis Mexico City using TROPOMI CO observations. *Atmos. Chem. Phys.* **2020**, *20*, 15761−15774.
(28) Varon, D. J.; Jacob, D. J.; McKeever, J.; Jervis, D.; Durak, B. O. A.; Xia, Y.; Huang, Y. Quantifying methane point sources from fine-scale satellite observations of atmospheric methane plumes. *Atmos. Meas. Tech.* **2018**, *11*, 5673−5686.
(29) Scarpelli, T. R.; Jacob, D. J.; Maasakkers, J. D.; Sulprizio, M. P.; Sheng, J.-X.; Rose, K.; Romeo, L.; Worden, J. R.; Janssens-Maenhout, G. A global gridded (0.1 × 0.1°) inventory of methane emissions from oil, gas, and coal exploitation based on national reports to the United Nations Framework Convention on Climate Change. *Earth Syst. Sci. Data* **2020**, *12*, 563−575.
(30) *National Inventory Report 2018—Volume 1*, Australian National Greenhouse Accounts, The Australian Government Submission to the United Nations Framework Convention on Climate Change, May 2020.
(31) Maasakkers, J. D.; Varon, D. J.; Elfarsdóttir, A.; McKeever, J.; Jervis, D.; Mahapatra, G.; Pandey, S.; Lorente, A.; Borsdorff, T.; Foorthuis, L. R.; Schuit, B. J.; Tol, P. J. J.; van Kempen, T. A.; van Hees, R. M.; Aben, I. Using satellites to uncover and evaluate large methane emissions from landfills, 2021. In preparation.
(32) Molod, A.; Takacs, L.; Suarez, M.; Bacmeister, J.; In-Sun, S.; Eichmann, A. *The GEOS-5 Atmospheric General Circulation Model: Mean Climate and Development from MERRA to Fortuna*; Technical Report Series on Global Modeling and Data Assimilation, Volume 28, 2012.
(33) Liu, Z.; Guan, D.; Wei, W.; Davis, S. J.; Ciais, P.; Bai, J.; Peng, S.; Zhang, Q.; Hubacek, K.; Marland, G.; Andres, R. J.; Crawford-Brown, D.; Lin, J.; Zhao, H.; Hong, C.; Boden, T. A.; Feng, K.; Peters, G. P.; Xi, F.; Liu, J.; Li, Y.; Zhao, Y.; Zeng, N.; He, K. Reduced carbon emission estimates from fossil fuel combustion and cement production in China. *Nature* **2015**, *524*, 335−338.
(34) Strong and Sustainable Resource Communities (SSRC), Queensland Government. https://dsdip.maps.arcgis.com/apps/webappviewer/index.html?id=77b3197acf5f415cb6f24553dd16b9dc (accessed March 21, 2021).
(35) Towler, B.; Firouzi, M.; Underschultz, J.; Rifkin, W.; Garnett, A.; Schultz, H.; Esterle, J.; Tyson, S.; Witt, K. An overview of the coal seam gas developments in Queensland. *J. Nat. Gas Sci. Eng.* **2016**, *31*, 249−271.
(36) *Estimating Emissions and Energy from Coal Mining Guideline*; National Greenhouse and Energy Reporting (NGER), Clean Energy Regulator, Australia Government, August 2020.
(37) Williams, D. J.; Saghafi, A.; Lange, A. L.; Drummond, M. S. *Methane Emissions from Open-Cut Mines and Post-Mining Emissions from Underground Coal*; Report to Department of Environment, Sports and Territories, CSIRO Investigation Report CET/IR173, 1993; p 17.
(38) Decision notice—Hail Creek Coal Mine Extension Transition Project; Department of the Environment and Energy (DEE), Australia Government. https://www.glencore.com.au/operations-and-projects/coal/current-operations/hail-creek-open-cut (accessed March 21, 2021).
(39) Fire Information for Resource Management System (FIRMS). https://firms2.modaps.eosdis.nasa.gov/map/#d:2021-04-21.2021-04-22;@0.0,0.0,3z (accessed March 21, 2021).

https://doi.org/10.1021/acs.est.1c03976
Environ. Sci. Technol. 2021, 55, 16573−16580